Journal of Medicinal Chemistry

pubs.acs.org/jmc

Article

Engineering of a Potent, Long-Acting NPY2R Agonist for Combination with a GLP-1R Agonist as a Multi-Hormonal Treatment for Obesity

Sam Lear,[§] Elsa Pflimlin,[§] Zhihong Zhou,[§] David Huang, Sharon Weng, Van Nguyen-Tran, Sean B. Joseph, Shane Roller, Scott Peterson, Jing Li, Matthew Tremblay, Peter G. Schultz, and Weijun Shen*

Cite This: https://dx.doi.org/10.1021/acs.jmedchem.0c00740

Read Online

ACCESS | Metrics & More | Article Recommendations | Supporting Information

ABSTRACT: Bariatric surgery results in increased intestinal secretion of hormones GLP-1 and anorexigenic PYY, which is believed to contribute to the clinical efficacy associated with the procedure. This observation raises the question whether combination treatment with gut hormone analogs might recapitulate the efficacy and mitigate the significant risks associated with surgery. Despite PYY demonstrating excellent efficacy and safety profiles with regard to food intake reduction, weight loss, and glucose control in preclinical animal models, PYY-based therapeutic development remains challenging given a low serum stability and half-life for the native peptide. Here, combined peptide stapling and PEG-fatty acid conjugation affords potent PYY analogs with >14 h rat half-lives, which are expected to translate into a human half-life suitable for once-weekly dosing. Excellent efficacy in glucose control, food intake reduction, and weight loss for lead candidate **22** in combination with our previously reported long-acting GLP-1 analog is demonstrated in a diet-induced obesity mouse model.

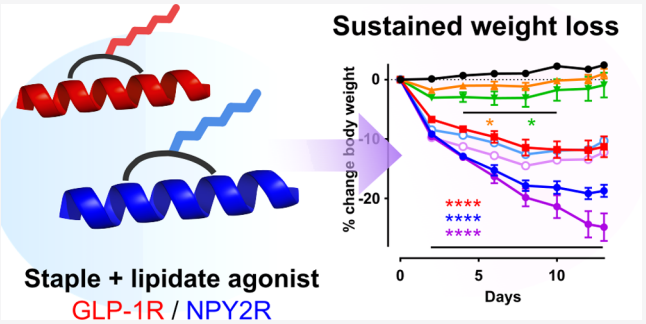

INTRODUCTION

The obesity epidemic is a major public health crisis and significant burden on healthcare systems worldwide.[1,2] Obesity is major risk factor for cardiovascular disease, musculoskeletal disorders, and cancers. In 2015, 12% of adults worldwide and over 30% of US adults were obese, with an estimated 4 million deaths attributed to high body mass index.[3] Thus, there is a clear unmet medical need for safe and effective weight loss therapies.[4] Bariatric surgery is currently the only effective therapeutic intervention for obesity that is demonstrated to produce a sustained weight loss effect, with the so-called *Roux-en-Y* gastric bypass accounting for the majority of all weight loss surgeries.[5] Furthermore, it is well established that changes in the secretion of numerous intestinal hormones, including peptide tyrosine tyrosine (PYY) and glucagon-like peptide-1 (GLP-1), occur following this type of surgery. It is these changes that are thought to play a significant role in the observed weight loss effect and enhancement of glycemic control,[6,5] which in some cases results in complete remission of type 2 diabetes.[7] Despite these highly positive results, bariatric surgery remains a highly invasive procedure, which is not without significant risk. PYY and GLP-1 when directly administered have shown excellent efficacy and safety profiles with regards to food intake reduction, weight loss, and glucose control.[5,8−16] However such therapies have not been fully realized, and while a limited number of PYY analogs have progressed into clinical trials,[17−19] no approved PYY-based drugs currently exist. While there has been some controversy regarding the anorexigenic and anti-obesity effects observed in rodent models following administration of PYY alone,[20,21] beneficial effects upon combination treatment with other peptide hormones have been demonstrated, and it is likely that this type of approach will be necessary to fully reverse the effects of obesity.[9,22] Indeed, improved efficacy through dosing of PYY analogs in combination with a GLP-1 receptor (GLP-1R) agonist as a second hormonal therapy has been established in animal models[23−25] and clinical obesity studies,[13,26−31] and such synergies likely stem from mimicking of the multi-hormonal effect of gastric bypass, crucially without the associated risks of surgical intervention.

Received: May 10, 2020

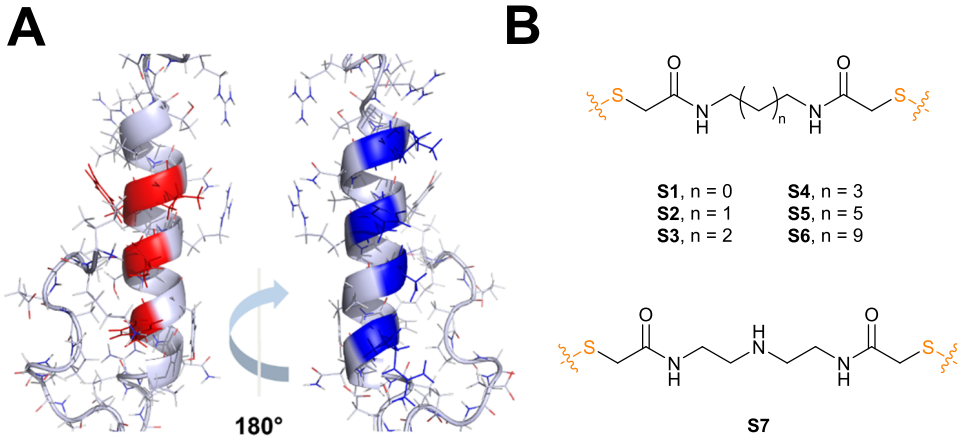

Figure 1. Structure of (A) neuropeptide Y bound to Y_2 receptor (NMR structure, receptor omitted; PDB ID: 2DF0),[47,48] with residues that interact with the receptor shown in red (Y20, L24, Y27, and L28) and those outside the binding pocket shown in blue (R19, S23, H26, and L30). (B) Structures of staples used for initial position/length screen, with (C) key peptide sequences.

Table 1. Optimization of Staple Position and Length for Stapled PYY Analogs (Activity Data for the Cellular NPY2R Activation Assay Shown)

		hNPY2R EC_{50} (nM)[a]					
sequence	cysteine substitutions	no staple	**S3** 10 atom	other staples			
PYY1	none	1.0 ± 0.1					
	i, *i* + 7						
PYY1	2, 9	2.9 ± 0.5	4.4 ± 0.5				
PYY1	10, 17	1.5 ± 0.3	4.8 ± 0.7	**S1** (8 atom)	6 ± 1	**S2** (9 atom)	8.1 ± 0.9
PYY1	17, 24	14 ± 2	4.3 ± 0.7				
PYY1	18, 25	740 ± 90	3 ± 1				
PYY1	19, 26	69 ± 7					
PYY1	20, 27	5 ± 1	5 ± 1				
PYY1	21, 28	190 ± 70	4 ± 2				
PYY1	22, 29	>10,000	14 ± 2				
PYY1	23, 30	6 ± 2	0.7 ± 0.8				
PYY1	24, 31	600 ± 300	160 ± 20				
	i, *i* + 11						
PYY1	10, 21	18 ± 2					
PYY1	13, 24	100 ± 10		**S5** (13 atom)	22 ± 3		
PYY1	19, 30	8 ± 4		**S5** (13 atom)	8 ± 6		
	i, *i* + 15						
PYY1	9, 24	23 ± 4		**S6** (17 atom)	32 ± 2		
PYY1	15, 30	8 ± 2		**S6** (17 atom)	15 ± 8		
PYY2	none	0.41 ± 0.03					
	i, *i* + 7						
PYY2	10, 17	0.32 ± 0.03	0.13 ± 0.01	**S4** (11 atom)	0.18 ± 0.02	**S7** (11 atom)	0.50 ± 0.05
PYY2	23, 30	0.32 ± 0.03	0.57 ± 0.04				

[a] EC_{50} determined in a cAMP reporter assay using CHO cells overexpressing human NPY2R in the presence of FBS (10%). Cells were treated with peptides in 12-point dose−response in culture medium with 10 μM forskolin as a positive control. The assay was carried out in triplicate for 30 min at 37 °C and 5% CO_2, and the cAMP detection kit from Cisbio was used to quantify cAMP accumulation.

A major challenge for such therapies is the lack of requisite serum stability and half-life for the native peptides, requiring high doses and frequent injection for chronic treatment. A variety of engineering strategies have been adopted in order to increase the potency and/or half-life of PYY, including backbone *N*-methylation and β-homo amino acid replace-

https://dx.doi.org/10.1021/acs.jmedchem.0c00740
J. Med. Chem. XXXX, XXX, XXX−XXX

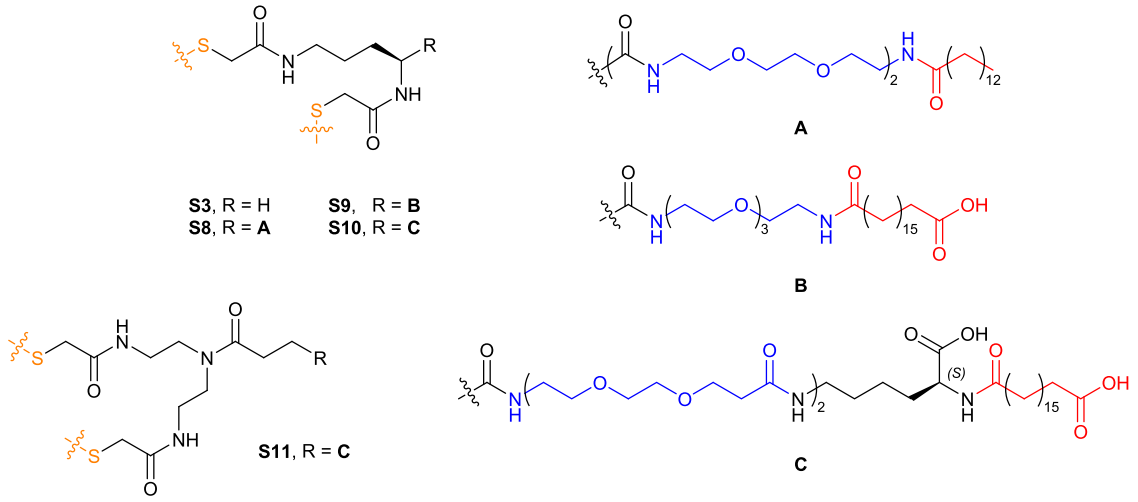

Figure 2. Structures of staples used for combined stapling and fatty acid conjugation.

ment,[32,33] other unnatural amino acid substitutions,[34−37] PEGylation,[38,39] and lipid[40,41] or antibody conjugation.[22] An additional consideration is the side effect of severe nausea observed upon clinical dosing of PYY and GLP-1 analogs, which poses a further challenge for clinical development.[13,24,38] A slow ramp up of exposure should mitigate this effect,[24] which is facilitated by a peptide with a suitably long half-life. To this end, we envisioned a PEG-fatty acid conjugated, stapled PYY analog with a human half-life suitable for once-weekly dosing. Furthermore, a synergistic enhancement in efficacy resulting from combination therapy with GLP-1 offers the possibility of a reduced dose of either peptide. Given our previously reported success in engineering the highly potent long-acting GLP-1R agonist "E6" (peptide **1**, see below)[42] with demonstrated *in vivo* efficacy in diabetes models, we explored an approach involving combination dosing of this peptide with an engineered NPY2R agonist with comparable pharmacokinetic profile. To this end, we combined peptide stapling and PEG-fatty acid conjugation to generate PYY analogs with high potency and long *in vivo* half-life, projected to translate to a human profile suitable for once-weekly dosing. Combination treatment with peptide **1** demonstrated superior glucose control, food intake reduction, and weight loss in a mouse model of diet-induced obesity and diabetes compared to either peptide alone.

RESULTS AND DISCUSSION

Staple Position Scanning and Length Optimization. Previously, we have shown that covalent modification of two engineered cysteine residues with a bis-bromoacetyl staple results in enhanced helicity and stability of alpha-helical peptide hormones.[42−46] The selection of stapling sites on PYY was guided by examination of the structure of the homologous neuropeptide Y (NPY) bound to human G protein-coupled neuropeptide Y receptor Y_2 (NPY2R, Figure 1).[47,48] Residues occurring on the face interacting with the receptor (Y20, L24, Y27, and L28) were avoided when choosing sites for covalent modification so as to minimize disruption of crucial peptide−receptor interactions. Rapid cleavage at the N-terminus of PYY by dipeptidyl peptidase-4 (DPP-4) following secretion results in the truncated peptide PYY_{3-36} ("PYY1" shown in Figure 1) being the predominant form in circulation.[10] As PYY1 shows higher specificity toward the Y_2 receptor subtype than PYY, we decided to use this truncated form for development as it is the Y_2 receptor specifically that mediates the anorectic effects of PYY analogs.[47] A set of PYY1 peptides was synthesized incorporating di-cysteine mutations at selected stapling positions representing a scan of the entire sequence and subsequently conjugated to bromoacetyl-functionalized staples using the solution-phase chemistry previously described.[42]

A scan of *i*, *i* + 7 diCys mutants was first carried out to find the best position in the sequence for stapling using the 10-atom staple **S3** (Figure 1), which we have previously demonstrated to be an appropriate length for effective *i*, *i* + 7 alpha-helix stapling.[42] To assess *in vitro* activity of the peptides and stapled analogs, we developed a cell-based NPY2R activation assay, where intracellular cAMP was quantified upon receptor activation in CHO cells over-expressing human NPY2R (see below and Experimental Section). Assay data are given in Table 1. Multiple diCys substitution positions were tolerated for unstapled PYY1 (2-9, 10-17, 20-27, and 23-30), typically with a loss in potency. However, stapling at position 23-30 with **S3** resulted in subnanomolar potency, similar to that of the native sequence (Figure 1). It was also anticipated that longer staples at *i*, *i* + 11 and *i*, *i* + 15 positions could potentially enhance the proteolytic stability of the peptides; however, stapling with the length-matched staples **S5** and **S6**, respectively, adversely affected activity. In addition, mutations were incorporated into the PYY1 sequence to further enhance potency of the native peptide (sequence "PYY2", Figure 1).[25] Given that both diCys incorporation and stapling at positions 10-17 and 23-30 resulted in the least overall loss of potency for PYY1, these 2 out of the initial 15 stapling positions were tested with the more active PYY2 sequence. Those PYY2 analogs stapled at the 10-17 and 23-30 positions were also found to be NPY2R agonists of equal, or in some cases enhanced, potency. Interestingly, staples **S4** and **S7** (which are slightly longer than **S3**) were also tolerated at position 10-17. Given this data, of the initial set of 36 analogs, two stapling positions (10-17 and 23-30) were taken forward in both PYY1 and PYY2 sequences to investigate fatty acid conjugation and incorporation of serum binding properties for enhanced half-life.

Fatty Acid Conjugation and Optimization. Next, we attached a PEG-fatty acid moiety onto the staple to enhance serum protein binding and extend half-life *in vivo*. A library of

https://dx.doi.org/10.1021/acs.jmedchem.0c00740
J. Med. Chem. XXXX, XXX, XXX−XXX

staples was synthesized incorporating a wide variety of PEG linker and fatty acid types, thus facilitating rapid screening of conjugates (Figure 2, synthesis detailed in the Supporting Information). Attachment of the bromoacetyl-functionalized staples to PYY1 and PYY2 sequences with Cys residues incorporated at the 10-17 and 23-30 positions was achieved in solution as previously described (1:1 ammonium bicarbonate buffer/acetonitrile, pH 8.5).[42] Ten-atom staples **S8-10** were initially tested due to the **S3** analogs being the most potent in the previous screen of unlipidated staples.

In vitro activity of the conjugates was assayed as described previously, and the results are summarized in Table 2. Activity

Table 2. *In Vitro* NPY2R Activation for Stapled PYY Analogs (*i*, *i* + 7) in the Presence (10%) and Absence (0%) of FBS in the cAMP Assay as Described Above [the Ratio between EC_{50} Values in the Presence or Absence of FBS Was Calculated as an Indicator of Serum Binding for a Variety of Fatty Acid Types/Chain Lengths (Selected Shown)]

				hNPY2R (cAMP)	
peptide	sequence	cysteine substitution(s)	staple	EC_{50} (nM) (0% FBS)	ratio 10:0% FBS
2	PYY1	none		1.2 ± 0.3	0.83
3	PYY1	10, 17	**S3**	2.7 ± 0.3	1.8
4	PYY1	10, 17	**S8**	2.3 ± 0.3	78
5	PYY1	10, 17	**S9**	22 ± 7	36
6	PYY1	10, 17	**S10**	44 ± 6	7.0
7	PYY1	23, 30	**S3**	1.0 ± 0.1	0.7
8	PYY1	23, 30	**S8**	1.2 ± 0.1	4.8
9	PYY1	23, 30	**S9**	3.1 ± 0.4	48
10	PYY1	23, 30	**S10**	40 ± 5	10
11	PYY2	none		0.29 ± 0.03	1.4
12	PYY2	10, 17	**S3**	0.18 ± 0.03	0.72
13	PYY2	10, 17	**S8**	0.62 ± 0.09	8.4
14	PYY2	10, 17	**S9**	0.85 ± 0.09	47
15	PYY2	10, 17	**S10**	1.2 ± 0.1	12
16	PYY2	23, 30	**S3**	0.65 ± 0.06	0.88
17	PYY2	23, 30	**S8**	0.44 ± 0.04	11
18	PYY2	23, 30	**S9**	0.91 ± 0.08	10
19	PYY2	23, 30	**S10**	3.7 ± 0.7	46

was first determined in the absence of serum to avoid any interference due to sequestration of the fatty acid-conjugated peptides by serum proteins such as serum albumin present in the assay. PYY2 demonstrated superior potency over the native PYY1 sequence as expected, observed previously for the unlipidated stapled analogs. In general, a large shift was observed between activity determined in the presence and absence of serum for staples **S9** and **S10**. This was attributed to enhanced serum binding *in vitro*, an effect previously shown to be indicative of longer *in vivo* half-life, observed for other commercially available lipidated peptide therapeutics such as semaglutide.[49] The peptide conjugates also showed good selectivity toward the NPY2R receptor over other receptor subtypes (Table 3), as expected for PYY analogs.[50] The majority of lipidated analogs were taken forward for determination of *in vivo* half-life (see below), selecting based on the best balance between absolute potency at 0% FBS and overall shift between 0% and 10% FBS assays, which was anticipated to provide the optimum serum binding and ideally the longest half-life. Based on these criteria, stapling of the

Table 3. *In Vitro* CRE Luciferase Assay Activity Data for PYY Analogs Demonstrating NPY Receptor Subtype Specificity (Experimental Details Given in the Experimental Section)

	EC_{50} (nM)			
peptide	NPY1R	NPY2R	NPY4R	NPY5R
2	2000	0.20 ± 0.06	7000	410 ± 90
11	>10,000	1.8 ± 0.4	>10,000	1200 ± 500
15	>10,000	0.3 ± 0.1	>10,000	>10,000

native PYY1 sequence at position 23-30 with **S9** appeared to afford the best profile in the *in vitro* assay, with **S9** stapling at position 10-17 being optimal for PYY2.

The "symmetric" staple **S11** (Figure 2) was also introduced to avoid the formation of regioisomers, which can occur upon stapling with **S10**. Activity for **S11**-stapled peptides was shown to be comparable to that of the corresponding **S10**-stapled analogs (Table 4). A clear serum shift was similarly observed

Table 4. *In Vitro* NPY2R Activation for PYY Analogs Stapled with "Symmetric" S11 in the cAMP Assay (as Described Above)

				hNPY2R (cAMP)	
peptide	sequence	cysteine substitution(s)	staple/ lipid	EC_{50} (nM) (0% FBS)	ratio 10:0% FBS
2	PYY1	none		1.2 ± 0.3	0.83
20	PYY1	23, 30	**S11**	7 ± 1	23
11	PYY2	none		0.29 ± 0.03	1.4
21	PYY2	10, 17	**S11**	0.65 ± 0.05	22
22	PYY2	23, 30	**S11**	5 ± 2	6.4

for **S11**-stapled **22**, as indicated by dose−response curves in the presence and absence of serum (Figure 3), implying enhanced serum binding and longer half-life *in vivo*.

***In Vivo* Half-Life.** The pharmacokinetic properties of the conjugates were assessed *in vivo* in order to determine the half-life extension effect of the fatty acid moiety (Table 5). Peptides in sterile saline were administered as a 1 h intravenous infusion to non-fasted male Sprague Dawley rats (n = 3) via femoral

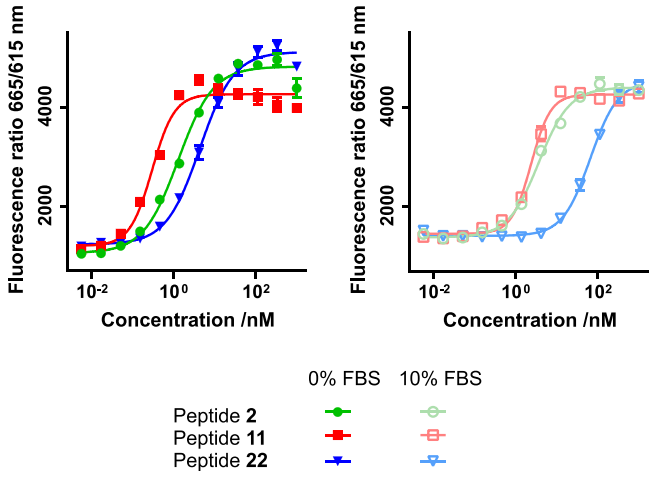

Figure 3. PYY analogs stapled with "symmetric" **S11**, with cAMP assay concentration−response curves in the presence and absence of fetal bovine serum (FBS).

https://dx.doi.org/10.1021/acs.jmedchem.0c00740
J. Med. Chem. XXXX, XXX, XXX−XXX

Table 5. *In Vivo* Pharmacokinetic Data for PYY Analogs

				hNPY2R (cAMP)		
peptide	sequence	cysteine substitution(s)	staple	EC_{50} (nM) (0% FBS)	ratio 10:0% FBS	rat $T_{1/2}$ (h)
4	PYY1	10, 17	**S8**	2.3 ± 0.3	78	INS
5	PYY1	10, 17	**S9**	22 ± 7	36	0.45
6	PYY1	10, 17	**S10**	44 ± 6	7.0	5.4
8	PYY1	23, 30	**S8**	1.2 ± 0.1	4.8	INS
9	PYY1	23, 30	**S9**	3.1 ± 0.4	48	2.4
10	PYY1	23, 30	**S10**	40 ± 5	10	3.9
11	PYY2	none		0.29 ± 0.03	1.4	1.2
13	PYY2	10, 17	**S8**	0.62 ± 0.09	8.4	INS
14	PYY2	10, 17	**S9**	0.85 ± 0.09	47	1.9
15	PYY2	10, 17	**S10**	1.2 ± 0.1	12	2.0
18	PYY2	23, 30	**S9**	0.91 ± 0.08	10	4.5
19	PYY2	23, 30	**S10**	3.7 ± 0.7	46	15
22	PYY2	23, 30	**S11**	5 ± 2	6.4	14

vein cannula at a final dose of 0.033 mg/kg. Blood samples were collected at 0.25, 0.5, 0.75, 1, 1.17, 1.33, 1.5, 2, 4, 6, 8, 24, 30, and 48 h after the start of infusion, and the plasma concentration of the peptides was analyzed via UPLC-MS/MS, as detailed in the Experimental Section. Despite the substantial serum shifts previously demonstrated for PYY1 conjugates, taken to be indicative of enhanced albumin binding, the longest *in vivo* half-lives observed were those for the PYY2 analogs. Furthermore, the predicted prolonged half-life for analogs stapled at the 10-17 position was not borne out in the *in vivo* data for either the PYY1 or PYY2 sequence, potentially due to stapling at this position not being protective against proteolytic degradation. While PYY2 stapling at position 10-17 retained the greatest activity *in vitro*, analogs stapled at position 23-30 had the longest half-lives, of up to 15 h in rat, which correlated with a large *in vitro* serum shift. For a given sequence and staple position, staples **S9-11**, all incorporating fatty acid moieties bearing carboxylic acid groups, were found to afford the most favorable pharmacokinetic properties, with **S10-11**, decorated with an "internal" carboxylate on the lysine linker, being superior (see Figure 2 for staple structures).

Although peptide **19** exhibited excellent *in vitro* potency and *in vivo* half-life, it was not taken forward due to the problem of regioisomer formation previously discussed for staple **S10**. A detailed pharmacokinetic profile for the longest-acting "symmetric" stapled analog **22** is shown in Figure 4. Peptide **22** exhibits a greater than 10-fold increase in half-life, with greatly reduced clearance when compared with the unstapled sequence (**11**). This profile is similar to the fatty acid-conjugated GLP-1R agonist semaglutide, which is dosed once-weekly in humans.[49] Given the long half-life observed for **22**, it was decided to take this peptide forward into food intake and body weight reduction models in mice in order to assess its *in vivo* efficacy.

Acute Food Intake Reduction Study in Wild-Type Mice. Given the well-established anorexigenic effect of PYY administration, a food intake study was carried out in C57BL/6 wild-type mice using peptide **22** at 0.04 and 0.2 mg/kg (8 and 40 nmol/kg) by subcutaneous injection (SC) (Figure 6). Peptide **22** was also tested in combination with a previously published long-acting GLP-1R agonist, peptide **1** (Figure 5).[42]

All groups show considerable reduction in food intake, with dosing of peptide **22** exhibiting a dose-dependent reduction in food consumption in the wild-type model. While peptide **1** dosed at 0.01 mg/kg (2 nmol/kg) shows comparable food

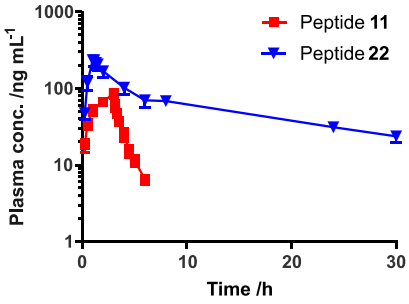

Peptide	Final dose /mg kg^{-1}	Infusion /h	CL /mL min^{-1} kg^{-1}	T_{max} /h	C_{max} /ng mL^{-1}	$T_{½}$ /h	AUC_{all} /h ng mL^{-1}
11	0.1	3	6.76	3.00	86.2	**1.21**	237
22	0.033	1	0.234	1.11	246	**14.4**	1870

Figure 4. Rat pharmacokinetic data: peptides in sterile saline were administered via intravenous (IV) infusion to non-fasted male Sprague Dawley rats (n = 3) via femoral vein cannula at the final dose shown. Blood samples were collected between 0.25 and 48 h after the start of infusion, and plasma concentration of the peptides was analyzed via UPLC-MS/MS, as detailed in the Experimental Section.

intake reduction to peptide **22** dosed at 0.04 mg/kg, the most robust food intake reduction effect was observed when 0.01 mg/kg **1** was used in combination with **22** at 0.04 and 0.2 mg/kg, resulting in a 64% and 90% reduction in cumulative food intake at 24 h, respectively. NPY2R agonists such as PYY_{3-36} and GLP-1R agonists such as exenatide and liraglutide are reported to slow gastric emptying and induce conditional taste aversion; therefore such effects are potentially responsible for the food intake reduction observed here for either agonist administered alone or in combination.[51,52] A single combined dose of peptide **1** and **22** (0.01 and 0.2 mg/kg, respectively) produced a significant body weight loss (~5%) observed at 48 h post dose, indicating a long-acting effect. With this preliminary data in hand, it was decided that the efficacy of both analogs (alone and in combination) should be assessed in a chronic body weight study.

Chronic Body Weight Reduction Study in Obese Mice. A 2-week chronic study to investigate the effect of daily administration of peptide **22** on body weight and glucose homeostasis, either alone or in combination with peptide **1**, was carried out in a diet-induced obesity (DIO) mouse model (Figure 7). The PYY analog (**22**) alone at 0.04 and 0.2 mg/kg

https://dx.doi.org/10.1021/acs.jmedchem.0c00740
J. Med. Chem. XXXX, XXX, XXX−XXX

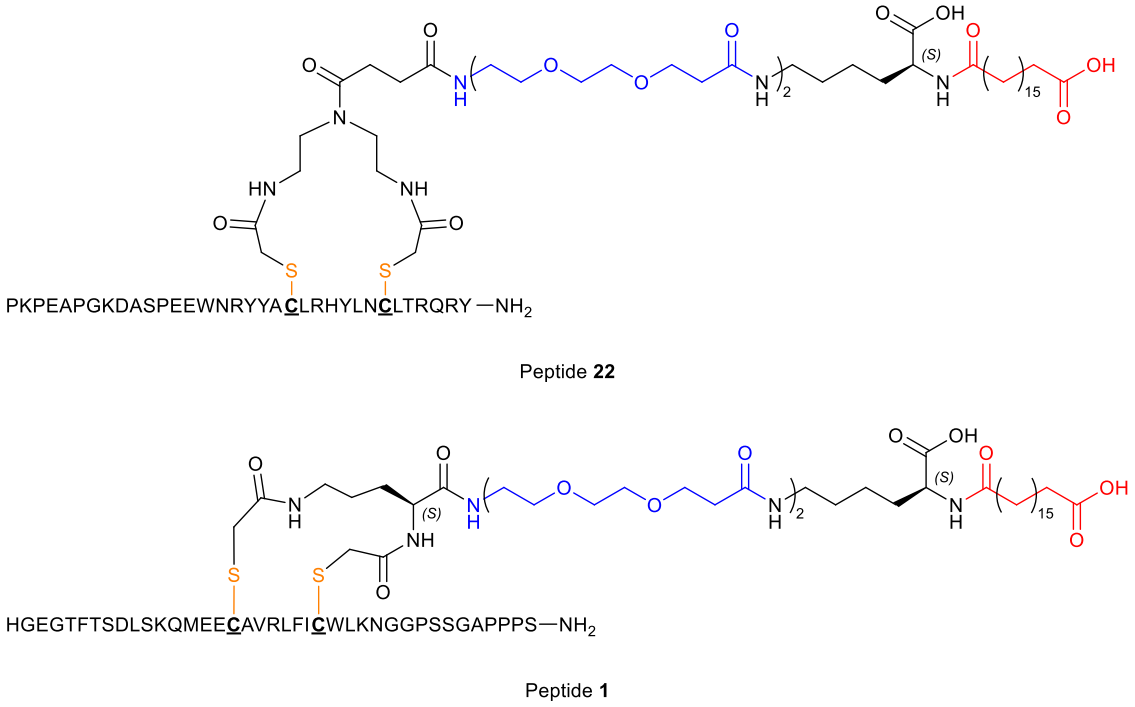

Figure 5. Full structures of peptides **1** and **22**.

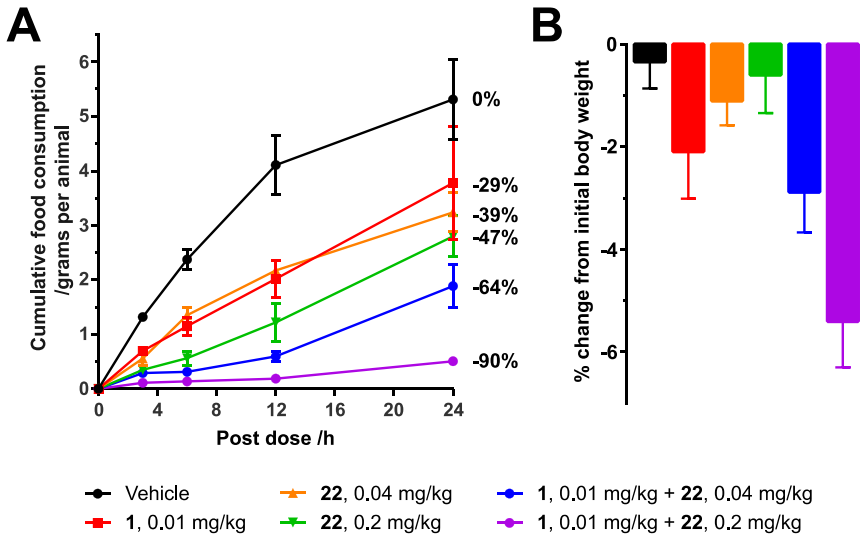

Figure 6. (A) Cumulative food intake in male C57BL/6 mice (n = 6 per group) over 24 h following a single SC dose of peptide or vehicle control (saline); % food intake inhibition relative to vehicle control at 24 h shown on the right side of the graph. (B) Acute change in body weight; % change from initial after 48 h.

demonstrated a dose-dependent reduction in food intake at day 1 compared to the vehicle control (Figure 7A), although this effect appeared to diminish over time (day 5, Figure 7B). As observed in the acute food intake study, peptide **1** alone was also efficacious; however, the most significant body weight reduction was demonstrated in both combination groups (Figure 7C). A dose of 0.01 mg/kg of peptide **1** in combination with the high dose (0.2 mg/kg) of peptide **22** resulted in nearly 25% body weight reduction after 13 days. Furthermore, body weight reduction in the combination groups substantially exceeded the predicted profile based on additive effects alone (expected additivity plotted), suggesting a synergistic enhancement of efficacy upon combination dosing. Similarly, the combination treatment demonstrated greater suppressive effects on food consumption compared to the GLP-1R agonist **1** alone after day 5 of dosing (Figure 7B).

Blood glucose homeostasis at day 14 was evaluated via the oral glucose tolerance test (OGTT, Figure 7D–F). Treatment with PYY analog **22** alone at either dose did not have a significant effect on the OGTT result or fasted blood glucose. While significant improvements were observed in the GLP-1R agonist (**1**) dosing groups, as expected,[42] the combination groups yielded slightly superior glucose control. The relatively modest glucose control effect demonstrated was not unexpected and is potentially due to the somewhat mild hyperglycemia observed in the prediabetic DIO model. A more pronounced effect may be observed upon longer treatment with the combination dose; however, the clear discrimination

https://dx.doi.org/10.1021/acs.jmedchem.0c00740
J. Med. Chem. XXXX, XXX, XXX−XXX

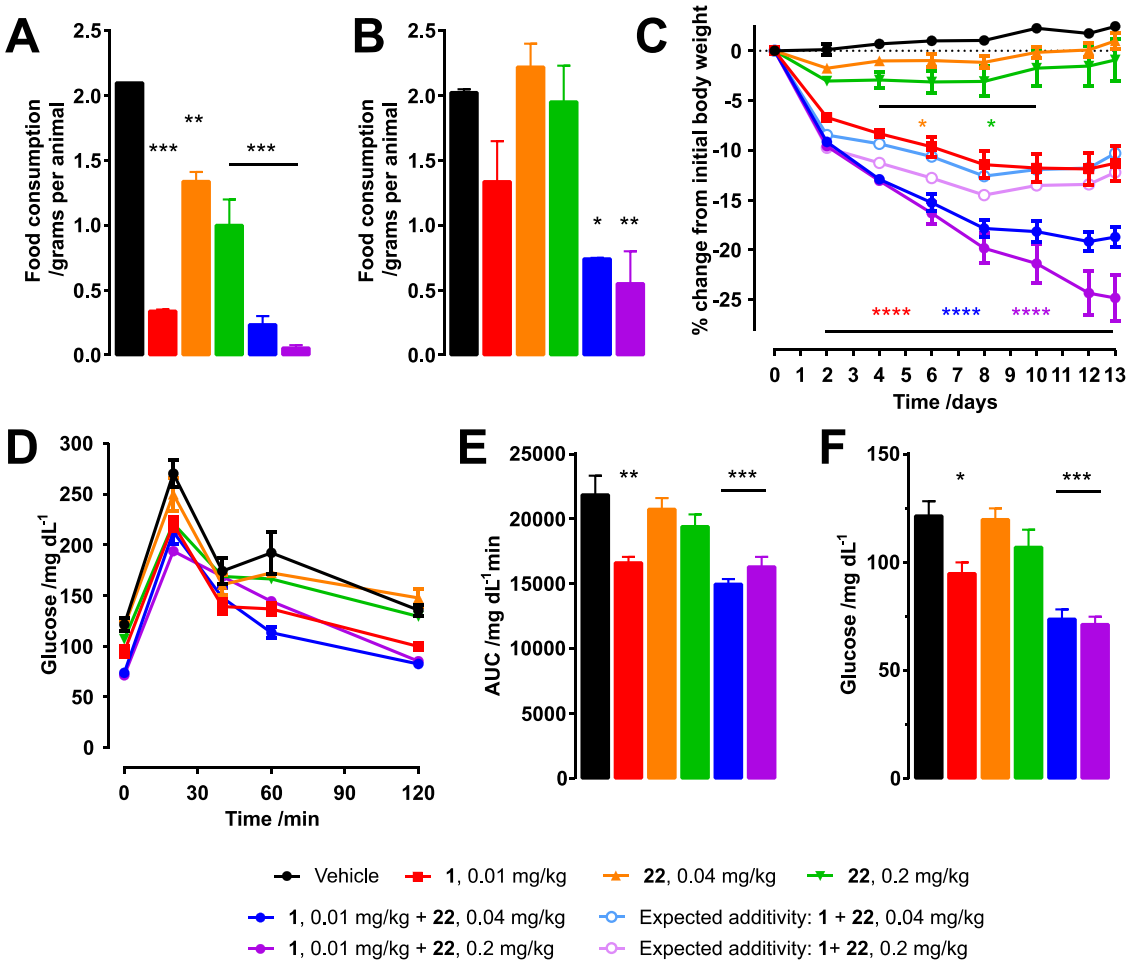

Figure 7. (A, B) Food consumption 12 h post dose (dark cycle) on (A) day 1 and (B) day 5 in male C57BL/6 DIO mice (n = 6 per group) with daily SC dosing of peptide or vehicle control (phosphate-buffered saline). (C) % change from initial body weight over 13 days. (D) Oral glucose tolerance test (OGTT) at day 14. (E) AUC for OGTT. (F) Fasted blood glucose at day 14. *P < 0.05, **P < 0.01, ***P < 0.001, ****P < 0.0001, relative to vehicle control [one-way ANOVA, or Student's t-test for (C)].

between those groups dosed with **1** and those without indicates that it is the effect of the GLP-1R agonist that is driving the glucose control effect in this study.

CONCLUSIONS

Bariatric surgery has proven to be the most effective, albeit risky, therapeutic intervention for obesity, providing immediate improvement in glucose control and a sustained reduction of body weight. Multi-hormonal therapies utilizing engineered, long-acting peptide hormones could pharmacologically recapitulate this effect. The peptide engineering strategy presented here, involving screening for optimal stapling sites followed by simultaneous stapling and PEG-fatty acid conjugation, affords potent long-acting PYY analogs. Peptide **22** in particular demonstrated a significantly extended half-life of 14 h in rat. Further *in vivo* studies revealed highly favorable food intake control and significant weight loss effect in a chronic efficacy study in combination with our previously discovered long-acting GLP-1R agonist **1**. Comparison to the approved peptide therapeutic semaglutide suggests that the observed rodent half-life is likely to translate to a projected pharmacokinetic profile in humans suitable for once-weekly dosing. Formulation optimization for peptide **22**, including stability and solubility screening, is ongoing. In our hands, **22** exhibits favorable solubility despite lipidation, which may be explained by reduced fibril formation compared to the unlipidated sequence, an effect previously reported for lipidated PYY analogs.[41] This approach serves as the starting point for the development of a clinical multi-hormone regimen designed to reverse the effects of obesity and rescue glycemic control. Furthermore, the engineering approach described is generally applicable to the translation of bioactive peptides into long-acting molecules suitable for pharmaceutical development and has found broad application in a variety of therapeutic areas.[42−46,53]

EXPERIMENTAL SECTION

No unexpected or unusually serious safety hazards were encountered. Unless otherwise noted, all reagents were purchased from commercial suppliers (Sigma Aldrich, Fisher, Oakwood) and used without further purification. Peptides were purchased from Cellmano Biotech Limited (Hefei), InnoPep (San Diego), Shanghai Apeptide Co. (Shanghai) or Shanghai Dechi Biosciences Co. (Shanghai). Staple **S11** was purchased from WuXi Apptec Co. (Shanghai). All reactions involving air- or moisture-sensitive reagents or intermediates were performed under an inert atmosphere of nitrogen or argon. All solvents used were of HPLC grade. Reactions were monitored by LC-MS or thin-layer chromatography (TLC) on Merck 50 × 100 mm silica gel 60 aluminum sheets stained using an aqueous solution of $KMnO_4$. Peptides were synthesized by standard solid-phase peptide synthesis (SPPS) techniques and purified via HPLC (as described below). Flash chromatography purifications were performed on silica gel

https://dx.doi.org/10.1021/acs.jmedchem.0c00740
J. Med. Chem. XXXX, XXX, XXX−XXX

prepacked columns (40 μm, RediSep Rf from Teledyne Isco) on a CombiFlash Rf (Teledyne Isco). Purified final compounds were eluted as single and symmetrical peaks (thereby confirming a purity of ≥95%). Semi-preparative chromatography were performed on a Shimadzu HPLC with a Phenomenex Luna column (C18, 100 Å pore size, 10 μm particle size, 250 × 10.0 mm, flow: 4 mL/min) or an Agilent 1200 HPLC with a Phenomenex Luna column (C18, 100 Å pore size, 5 μm particle size, 150 × 21.2 mm, flow: 20 mL/min). ^{1}H and ^{13}C NMR spectra were recorded on a Bruker 400 system in DMSO-d_6, $CDCl_3$, or CD_3OD. Chemical shifts are given in parts per million (ppm) with tetramethylsilane as an internal standard. Abbreviations are used as follows: s = singlet, d = doublet, t = triplet, q = quartet, p = pentet, m = multiplet, dd = doublet of doublets, br = broad. Coupling constants (J values) are given in hertz (Hz). Low-resolution mass spectra were recorded on a Waters Acquity UPLC with a Phemomenex Luna Omega C18 column (C18, 100 Å pore size, 1.6 μm particle size, 50 × 2.1 mm, flow: 0.4 mL/min). Solvents: A, H_2O + 0.1% formic acid; B, MeCN + 0.1% formic acid; gradient: 0−1 min 10−90% B, 1−1.6 min 90% B, 1.6−1.7 min 90−10% B, and 1.7−2 min 10% B. High-resolution mass spectra (HRMS) were recorded on an Agilent 1200 Series Accurate Mass Time-of-Flight (TOF) with an Aeris Widepore column (XB-C8, 3.6 μm particle size, 150 × 2.1 mm, flow: 0.5 mL/min). Solvents: A, H_2O + 0.1% formic acid; B, MeCN + 0.1% formic acid; gradient: 0−2 min 5% B, 2−12 min 5−60% B, 12−13 min 60−80% B, 13−14 min 80−20% B, 14−15 min 20−80% B, 15−16 min 80−20% B, 16−17 min 20−95% B, 17−20 min 95% B, and 20−21 min 95−5% B.

General Procedure for Bromoacetyl Peptide Stapling/Conjugation. Peptides were dissolved at a concentration of 2 mM with 1.5 equiv of bromoacetyl staple in 1:3 (v/v) MeCN/30 mM NH_4HCO_3 buffer (pH 8.5). The pH of the reaction mixture was readjusted with ammonium hydroxide to correct the drop in pH caused by the peptide TFA counterion. More MeCN was added for particularly insoluble peptides. The reaction was stirred at RT for 2−4 h before acidification to pH 5 via dropwise addition of acetic acid. The resulting solution was lyophilized and purified by reversed-phase HPLC.

Synthesis of Staples S2-6 and S8-10. Synthesis of staples **S2** and **S4-6**[42] and **S3** and **S8-10**[42,43,45] was carried out as previously reported. Briefly, staples **S2-6** were synthesized via coupling of the corresponding diamine and bromoacetic anhydride in solution and used directly for stapling without further purification. Fatty acid-containing staples **S8-10** were synthesized using commercially available building blocks as follows: **S8**, coupling of the fatty acid and mono-Boc-protected diamino-PEG in solution followed by sequential Boc deprotection (TFA/DCM) and coupling of Boc-NH-PEG_2-OH then Boc-Orn(Boc)-OH followed by final Boc deprotection and bromoacetylation of free ornithine amine groups using bromoacetic anhydride; the final staple was purified using flash column chromatography, as described; **S9**, coupling of Boc-Orn-(Boc)-OH and amino-PEG_3-azide in solution followed by reduction of azide (H_2, Pd/C), coupling of mono-*t*Bu-protected fatty diacid followed by final Boc deprotection and bromoacetylation;, the final staple was purified using flash column chromatography, as described; **S10**, sequential solid-phase coupling of Fmoc-Lys(ivDde)-OH and mono-*t*Bu-protected fatty diacid to chlorotrityl chloride resin (protocols A, B, and D below), ivDde deprotection (protocol C below), sequential coupling of Fmoc-NH-PEG_2-OH and Fmoc-Orn(Fmoc)-OH (protocols B and D below), deprotection of ornithine Fmoc groups (protocol B below), and on-resin bromoacetylation (protocol E below) and cleavage from the solid support (protocol F below); the final staple was purified using reversed-phase HPLC, as described.

General Solid-Phase Synthesis Protocols for Staples S10 and S11. *Loading of Chlorotrityl Chloride Resin (A).* Fmoc-Lys(ivDde)-OH (60 mg, 100 μmol) was coupled to 2-chlorotrityl chloride resin (Novabiochem) (100 mg, 80 μmol) by mixing the amino acid, resin, and DIEA (70 μL, 400 μmol) in 5 mL of DMF and stirring for 30 min. The resin was then washed with DMF (3x) and DCM (3x) and treated with CH_3OH/DCM/DIEA (8:1:1) for 10 min to cap the unreacted trityl chloride sites, dried under vacuum, and stored in a desiccator.

Deprotection of Fmoc Protecting Group (B). To the resin was added piperidine in DMF (20%). The mixture was shaken for 5 min and drained. Fresh 20% piperidine was added, and this time the mixture was shaken for 15 min. Positive ninhydrin and/or TNBS test was observed. The resin was then washed with DMF (3x), DCM (3x).

Deprotection of ivDde Protecting Group (C). After washing with DMF and DCM, the resin was treated with 2% hydrazine in DMF (5 mL, 2 × 15 min). Positive ninhydrin and/or TNBS test was observed. The resin was then washed with DMF (3x) and DCM (3x).

Peptide Coupling (D). The resin was treated with the carboxylic acid derivative specified (3 equiv) using coupling reagent HATU (3.3 eq) and DIEA (3.3 eq) in DMF (5 mL) for 2 h or repeated until a negative ninhydrin and/or TNBS test was observed. The resin was then washed with DMF (3x) and DCM (3x).

On-Resin Bromoacetylation (E). The resin was then treated with bromoacetic anhydride (2.4 equiv) and DIEA (2.6 equiv) in 200 mL of DCM for 30 min.

Cleavage of Peptides from Chlorotrityl Resin (F). The resin was washed with DCM (3x), and the product was cleaved from the resin using 5 mL of 10% TFA in DCM containing 10% H_2O and 10% triisopropylsilane for 1 h.

***N,N′*-(Ethane-1,2-diyl)bis(2-bromoacetamide) (S1).**

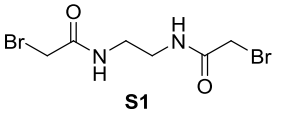

S1

To a solution of 1,2-ethylenediamine (30 μL, 0.448 mmol, 1 equiv) in DCM (5 mL) at 0 °C were added DIEA (172 μL, 0.985 mmol, 2.2 equiv) followed by bromoacetic anhydride (233 mg, 0.897 mmol, 2 equiv) dissolved in 1 mL of DCM. The reaction mixture was then stirred for 30 min at 0 °C, 1.5 h at RT, and the solvent was removed. Purification by flash column chromatography on silica gel provided **S1** as a white solid (43.9 mg, 0.145 mmol, 32%); MS (ES^+) m/z 302.55 ($[M + H]^+$), 304.54 ($[M + H]^+$); ^{1}H NMR (400 MHz, methanol-d_4) δ 2.49 (s, 4H), 2.06 (s, 4H).

***N,N′*-(Azanediylbis(ethane-2,1-diyl))bis(2-bromoacetamide) (S7).** *Intermediate **S7a**.*

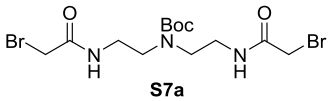

S7a

To a solution of *tert*-butyl bis(2-aminoethyl)carbamate (167 mg, 0.82 mmol, 1 equiv) in DCM (20 mL) at 0 °C were added DIEA (342 μL, 11.96 mmol, 2.4 equiv) followed by bromoacetic anhydride (426 mg, 1.64 mmol, 2 equiv) dissolved in 1 mL of DCM. The reaction mixture was then stirred for 30 min at 0 °C, 1.5 h at RT, and the solvent was removed. Purification by flash column chromatography on silica gel afforded **S7a** as a white solid (289 mg, 0.65 mmol, 79%); MS (ES^+) m/z 445.71 ($[M + H]^+$), 447.7 ($[M + H]^+$); ^{1}H NMR (400 MHz, methanol-d_4) δ 3.85 (s, 4H), 3.39 (s, 9H), 1.50 (s, 10H).

***S7*.**

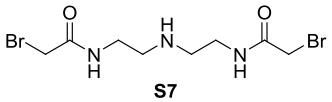

S7

Compound **S7a** (20 mg) was dissolved in TFA/DCM (1:1, v/v, 2 mL), agitated 30 min at RT, and evaporated (co-evaporation with hexane) to obtain compound **S7** as an oil. The product was directly used in further steps; MS (ES^+) m/z 345.2 ($[M + H]^+$).

(*S*)-1-Bromo-6-(2-(2-bromoacetamido)ethyl)-36-carboxy-2,7,10,20,30,38-hexaoxo-14,17,24,27-tetraoxa-3,6,11,21,31,37-hexaazapentapentacontan-55-oic Acid (S11). *Intermediate **S11a**.*

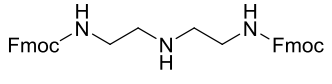

S11a

https://dx.doi.org/10.1021/acs.jmedchem.0c00740
J. Med. Chem. XXXX, XXX, XXX−XXX

A solution of Fmoc-OSu (131 g, 388 mmol) in DCM (200 mL) was added dropwise to a solution of diethylenetriamine (20 g, 194 mmol) in DCM (200 mL) at −40 °C under N_2 and stirred for 2 h. LC-MS showed that the reaction was complete. The crude product in solution was not purified and used for the next step directly; ^{1}H NMR (400 MHz, DMSO-d_6) δ 7.88 (d, J = 7.6 Hz, 4H), 7.68 (d, J = 7.6 Hz, 4H), 7.43−7.24 (m, 10H), 4.30 (d, J = 6.4 Hz, 4H), 4.21 (d, J = 6.4 Hz, 2H), 3.06 (d, J = 5.6 Hz, 4H), 2.57 (d, J = 7.6 Hz, 4H); MS (ES$^+$) m/z 548.2 ([M + H]$^+$).

Intermediate ***S11b***.

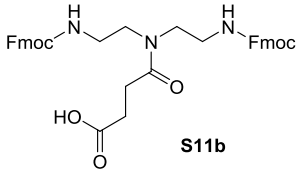

S11b

To a solution of compound **S11a** (106 g, 194 mmol) in DCM (400 mL) was added DMAP (4.74 g, 38.8 mmol) and tetrahydrofuran-2,5-dione (67.9 g, 678 mmol) and stirred at 25 °C for 14 h. LC-MS showed that the reaction was complete. To the reaction mixture was added 1 N HCl until pH = 5−6 and stirred for 15 min, the organic phase was separated, then the organic phase was washed with water and saturated NaCl (500 mL) and the aqueous phase was extracted with DCM (500 mL) twice. The combined DCM was dried over anhydrous Na_2SO_4 and concentrated under vacuum. The crude product was purified by column chromatography on silica gel using DCM/MeOH (80:0−5:1) as an eluent to give compound **S11b** (57.6 g, 45% yield) as a white solid powder; ^{1}H NMR (400 MHz, DMSO-d_6) δ 12.09 (s, 1 H), 7.87 (d, J = 7.5 Hz, 4 H), 7.66 (d, J = 7.0 Hz, 4 H), 7.23−7.48 (m, 10 H), 4.24−4.33 (m, 4 H), 4.14−4.22 (m, 2 H), 3.27 (s, 4 H), 2.95−3.19 (m, 4 H), 2.37−2.44 (m, 4 H); MS (ES$^+$) m/z 648.2 ([M + H]$^+$).

S11 *(Figure 2)*. General protocols **A**, **B**, **D** (octadecanedioic acid mono-*tert*-butyl ester), **C**, **D** (Fmoc-PEG_2-propionic acid), **B**, **D** (Fmoc-PEG_2-propionic acid), **B**, **D** (compound **S11b**), and **B**, **E**, **F**. The crude was purified by HPLC to afford the product **S11** as a white solid (5.2 g, 11% yield); MS (ES$^+$) m/z 1188.5 ([M + H]$^+$).

In Vitro **Assays.** *Intracellular cAMP Assay.* To measure peptide-induced NPY2R-mediated inhibition of cAMP production, a cAMP HTRF (cyclic adenosine monophosphate homogeneous time-resolved fluorescence) assay was performed according to the manufacturer's instructions (cAMP, Gs Dynamic kit, Cisbio). Briefly, cAMP Hunter CHO cells expressing the NPY2R (DiscoveRx) were seeded overnight in white 384-well plates at 5000 cells per well in 20 μL of F12 medium at 37 °C and 5% CO_2. The following day, the medium was removed and replaced with 20 μL of Opti-MEM (Gibco) in the presence or absence of 10% FBS. Peptides (prepared as 5X solution in Opti-MEM) at 12 different concentrations in triplicate and forskolin (a direct activator of adenylate cyclase enzyme, final concentration of 10 μM) were added and incubated for 30 min at 37 °C. Detection reagent was added and further incubated for 60 min at room temperature and read on a compatible HTRF reader (PHERAstar). The EC_{50} of each peptide was determined using GraphPad Prism 6 software (GraphPad, San Diego, CA). Average EC_{50} and standard deviation (SD) for each peptide were derived from three independent experiments.

CRE-Luciferase Reporter Assay. HEK293 cells were infected with lentivirus encoding firefly luciferase gene under the control of cAMP responsive element (CRE) promoter (Qiagen, Netherlands) and then were selected using 1 μg/mL puromycin (Life Technologies, Carlsbad) for 1 week. The surviving cells (referred to as CRE-HEK293) were expanded and then transfected with a G418 selective mammalian expression plasmid encoding human NPY2R. The NPY2R plasmid was transfected into CRE-HEK293 cells using Lipofectamine 2000 and selected with 400 μg/mL geneticin (Life Technologies, Carlsbad, CA). A single colony stable cell line overexpressing both CRE-luciferase and NPY2R (HEK293-NPY2R-CRE) was then established for the *in vitro* activity assay. HEK293-NPY2R-CRE cells were seeded in 384-well plates at a density of 5000 cells per well and cultured for 18 h in DMEM with 10% FBS at 37 °C and 5% CO_2. Cells were treated with peptide at 12 different concentrations in triplicate for 24 h and receptor activation was reported by luminescence intensities using One-Glo (Promega, WI) luciferase reagent as per the manufacturer's instructions. The EC_{50} of each peptide was determined using GraphPad Prism 6 software (GraphPad, San Diego, CA). Average EC_{50} and standard deviation (SD) for each peptide were derived from three independent experiments.

Animal Studies. All animal care and experimental procedures were approved by the Intarcia Testing Facility Institutional Animal Care and Use Committee (IACUC) or the IACUC of the California Institute for Biomedical Research (Calibr) and strictly followed the NIH guidelines for humane treatment of animals.

In Vivo **Pharmacokinetic (PK) Study.** Peptides were dissolved in sterile saline and administered as a 1 h intravenous infusion to non-fasted male Sprague Dawley rats, age 9−20 weeks (median 14 weeks), body weight 369−554 g (median 460 g) from Charles River Laboratories (Raleigh, NC), via femoral vein cannula at a final dose of 0.033 mg/kg (n = 3 per compound). All cannulas were externalized via a three-port Instech vascular access button (Instech Laboratories, Inc., Plymouth Meeting, PA) located in the rear midscapular region. Formulations were administered at a rate of 1.67 mL/kg/h. All animals were singly housed in DiLab caging with free access to food and water for the duration of the study. Ambient temperature and humidity were maintained in the study room. The light cycle consisted of 12 h of light followed by 12 h of darkness. All animals appeared healthy prior to the start of dosing. Blood samples (approximately 250 μL) were collected for pharmacokinetic analysis via a jugular vein cannula at 0.25, 0.5, 0.75, 1, 1.17, 1.33, 1.5, 2, 4, 6, 8, 24, 30, and 48 h post-start of infusion into microtainer tubes containing K_2EDTA as an anticoagulant and 25 μL of a protease inhibitor cocktail. Plasma was prepared by centrifugation and stored at −80 °C until analysis.

PK Plasma Sample Preparation. An aliquot of each plasma sample was placed into to a 96-well plate. To each well, Tween-20 was added to a final concentration of 0.05%. Plates were then vortex mixed before three volumes of 0.1% TFA in 2:1 ethanol:acetonitrile containing an appropriate internal standard was added to each well. Plates were vortex mixed again and then centrifuged for 10 min at 2844*g*. Supernatants were placed into a clean 96-well plate and evaporated under a nitrogen stream at 45 °C. Residues were reconstituted in 20% acetonitrile (aq) containing 0.1% formic acid.

LC-MS Quantification of Peptides in Plasma. All calibration standards were prepared in control rat plasma containing K_2EDTA and protease inhibitor cocktail. Samples and standards were analyzed by TurboIonSpray UPLC-MS/MS using a system consisting of a CTC HTS PAL auto-injector (Leap, Carrboro, NC), an Agilent Infinity 1290 system with column oven (Palo Alto, CA), a Valco switching valve (Houston, TX), and either an AB Sciex API 5600 TripleTOF or Sciex API 4000QTrap mass spectrometer (Framingham, MA). Samples were injected onto a 2.1 × 50 mm reverse phase C18 analytical column, typically a Waters ACQUITY UPLC HSS T3, 1.8 μm (Waters Corporation, Milford, MA) or similar. Chromatographic separation was achieved with a gradient method using water containing 0.1% formic acid (A) and acetonitrile containing 0.1% formic acid (B) as a mobile phase. Initial conditions consisted of 95% A and 5% B. The organic component was increased to 95% B over a period of 3−4 min, depending on the peptide. Typical flow rates were 600 μL/min. The column temperature was held constant at 40 or 45 °C. Peptides were quantified my monitoring one or more product ions produced from a multiply charged parent ion.

Wild-Type Mouse Food Intake Model. C57BL/6 wild-type male mice (age 15 weeks from Jackson Labs, Bar Harbor, ME) maintained on regular chow diet were acclimated in reverse light cycle and administered a single dose of peptide (5 mL/kg) by subcutaneous injection (n = 6, group housed 2 mice per cage). Food intake was monitored at 0 (beginning of the dark cycle), 3, 6, 12, and 24 h and body weight at 0 and 48 h post dose.

https://dx.doi.org/10.1021/acs.jmedchem.0c00740
J. Med. Chem. XXXX, XXX, XXX−XXX

Diet-Induced Obesity (DIO) Mouse Body Weight Model. C57BL/6 diet-induced obesity (DIO) model male mice (age 18 weeks from Jackson Labs, Bar Harbor, ME) maintained on high fat diet (D12492, 60% fat diet) for 12 weeks were administered a peptide by daily subcutaneous injection for up to 13 days (n = 6, group housed 2 mice per cage, regular light cycle). The average body weight at the beginning of the experiment was 50 g. Mouse body weight was measured on days 0, 2, 4, 6, 8, 10, 12, and 13. Mice were fasted overnight prior to the oral glucose tolerance test (OGTT) on day 14 and then dosed with peptide. After 6 h, 1 g of glucose solution per kg body weight was administered orally, and mouse tail blood glucose levels were measured before (0 min) and after glucose challenge for 2 h. The data were compared using the unpaired Student's t-test. Where appropriate, data were compared using repeated measures or one-way analysis of variance followed by the Student–Newman–Keuls post hoc test.

■ ASSOCIATED CONTENT

Supporting Information

The Supporting Information is available free of charge at https://pubs.acs.org/doi/10.1021/acs.jmedchem.0c00740.

Listing of stapled peptides, HPLC and MS data for peptides, and chronic DIO study initial body weight data (PDF)

PDB ID: 2DF0 (PDB)

■ AUTHOR INFORMATION

Corresponding Author

Weijun Shen − *The Scripps Research Institute, d/b/a Calibr, a division of Scripps Research, La Jolla, California 92037, United States;* orcid.org/0000-0001-8388-729X; Email: wshen@scripps.edu

Authors

Sam Lear − *The Scripps Research Institute, d/b/a Calibr, a division of Scripps Research, La Jolla, California 92037, United States*

Elsa Pflimlin − *The Scripps Research Institute, d/b/a Calibr, a division of Scripps Research, La Jolla, California 92037, United States*

Zhihong Zhou − *The Scripps Research Institute, d/b/a Calibr, a division of Scripps Research, La Jolla, California 92037, United States*

David Huang − *The Scripps Research Institute, d/b/a Calibr, a division of Scripps Research, La Jolla, California 92037, United States*

Sharon Weng − *Intarcia Therapeutics, Inc., Durham, North Carolina 27709, United States*

Van Nguyen-Tran − *The Scripps Research Institute, d/b/a Calibr, a division of Scripps Research, La Jolla, California 92037, United States*

Sean B. Joseph − *The Scripps Research Institute, d/b/a Calibr, a division of Scripps Research, La Jolla, California 92037, United States*

Shane Roller − *The Scripps Research Institute, d/b/a Calibr, a division of Scripps Research, La Jolla, California 92037, United States*

Scott Peterson − *Intarcia Therapeutics, Inc., Durham, North Carolina 27709, United States*

Jing Li − *The Scripps Research Institute, d/b/a Calibr, a division of Scripps Research, La Jolla, California 92037, United States*

Matthew Tremblay − *The Scripps Research Institute, d/b/a Calibr, a division of Scripps Research, La Jolla, California 92037, United States;* orcid.org/0000-0002-9906-0219

Peter G. Schultz − *The Scripps Research Institute, d/b/a Calibr, a division of Scripps Research, La Jolla, California 92037, United States;* orcid.org/0000-0003-3188-1202

Complete contact information is available at: https://pubs.acs.org/10.1021/acs.jmedchem.0c00740

Author Contributions

§S.L., E.P., and Z.Z. contributed equally to this work.

Notes

The authors declare no competing financial interest.

■ ACKNOWLEDGMENTS

We would like to thank Huafei Zou and Qiangwei Fu for technical support and useful discussions.

■ ABBREVIATIONS USED

ANOVA, analysis of variance; AUC, area under the curve; cAMP, cyclic adenosine monophosphate; CHO, Chinese hamster ovary; CL, clearance; C_{max}, maximum serum concentration; CRE, cAMP responsive element; DCM, dichloromethane; DIEA, *N*,*N*-diisopropylethylamine; DIO, diet-induced obesity; DMAP, 4-dimethylaminopyridine; DMF, dimethylformamide; DMSO, dimethyl sulfoxide; DPP-4, dipeptidyl peptidase-4; EC_{50}, half maximal effective concentration; EDTA, ethylenediaminetetraacetic acid; ES, electrospray; FBS, fetal bovine serum; Fmoc, fluorenylmethyloxycarbonyl; GLP-1, glucagon-like peptide-1; GLP-1R, GLP-1 receptor; HATU, 1-[bis(dimethylamino)methylene]-1*H*-1,2,3-triazolo[4,5-*b*]pyridinium 3-oxid hexafluorophosphate; hNPY2R, human NPY2R; HPLC, high-performance liquid chromatography; HRMS, high-resolution mass spectra; HTRF, homogeneous time-resolved fluorescence; IACUC, Institutional Animal Care and Use Committee; INS, insignificant (half-life too short to be measured); IV, intravenous; ivDde, 1-(4,4-dimethyl-2,6-dioxocyclo-hexylidene)-3-methylbutyl; LC-MS, liquid chromatography–mass spectrometry; MS, mass spectrometry; MS/MS, tandem mass spectrometry; NMR, nuclear magnetic resonance; NPY, neuropeptide Y; NPY2R, neuropeptide Y receptor Y_2; OGTT, oral glucose tolerance test; Orn, ornithine; OSu, *N*-hydroxysuccinimide ester; PDB, Protein Data Bank; PEG, polyethylene glycol; PK, pharmacokinetic; PYY, peptide tyrosine tyrosine; RT, room temperature; SC, subcutaneous; SPPS, solid-phase peptide synthesis; $T_{1/2}$, half-life; TFA, trifluoroacetic acid; TLC, thin-layer chromatography; T_{max}, time at C_{max}; TNBS, 2,4,6-trinitrobenzenesulfonic acid; TOF, time-of-flight; UPLC, ultra-performance liquid chromatography

■ REFERENCES

(1) Kearns, K.; Dee, A.; Fitzgerald, A. P.; Doherty, E.; Perry, I. J. Chronic Disease Burden Associated with Overweight and Obesity in Ireland: The Effects of a Small BMI Reduction at Population Level. *BMC Public Health* **2014**, *14*, 143.

(2) Mitchell, N. S.; Catenacci, V. A.; Wyatt, H. R.; James, O. H. Obesity: Overview of an Epidemic. *Psychiatric Clin.* **2011**, *34*, 717–732.

(3) Afshin, A.; Forouzanfar, M. H.; Reitsma, M. B.; Sur, P.; et al. Health Effects of Overweight and Obesity in 195 Countries Over 25 Years. *N. Engl. J. Med.* **2017**, *377*, 13–27.

(4) Arbeeny, C. M. Addressing the Unmet Medical Need for Safe and Effective Weight Loss Therapies. *Obes. Res.* **2004**, *12*, 1191–1196.

https://dx.doi.org/10.1021/acs.jmedchem.0c00740
J. Med. Chem. XXXX, XXX, XXX–XXX

(5) Troke, R. C.; Tan, T. M.; Bloom, S. R. The Future Role of Gut Hormones in the Treatment of Obesity. *Ther. Adv. Chronic Dis.* **2014**, *5*, 4−14.
(6) Guida, C.; Stephen, S. D.; Watson, M.; Dempste, N.; Larraufie, P.; Marjot, T.; Cargill, T.; Rickers, L.; Pavlides, M.; Tomlinson, J.; Cobbold, J. F. L.; Zhao, C.-M.; Chen, D.; Gribble, F.; Reimann, F.; Gillies, R.; Sgromo, B.; Rorsmana, P.; Ryan, J. D.; Ramracheya, R. D. PYY Plays a Key Role in the Resolution of Diabetes Following Bariatric Surgery in Humans. *EBioMedicine* **2019**, *40*, 67−76.
(7) Koliaki, C.; Liatis, S.; le Roux, C. W.; Kokkinos, A. The Role of Bariatric Surgery to Treat Diabetes: Current Challenges and Perspectives. *BMC Endocr. Disord.* **2017**, *17*, 50.
(8) Gribble, F. M.; Reimann, F. Function and Mechanisms of Enteroendocrine Cells and Gut Hormones in Metabolism. *Nat. Rev. Endocrinol.* **2019**, *15*, 226−237.
(9) Clemmensen, C.; Finan, B.; Müller, T. D.; DiMarchi, R. D.; Tschöp, M. H.; Hofmann, S. M. Emerging Hormonal-Based Combination Pharmacotherapies for the Treatment of Metabolic Diseases. *Nat. Rev. Endocrinol.* **2019**, *15*, 90−104.
(10) Lafferty, R. A.; Flatt, P. R.; Irwin, N. Emerging Therapeutic Potential for Peptide YY for Obesity-Diabetes. *Peptides* **2018**, *100*, 269−274.
(11) Meneguetti, B. T.; Cardoso, M. H.; Ribeiro, C. F. A.; Felício, M. R.; Pinto, I. B.; Santos, N. C.; Carvalho, C. M. E.; Franco, O. L. Neuropeptide Receptors as Potential Pharmacological Targets for Obesity. *Pharmacol. Ther.* **2019**, *196*, 59−78.
(12) Perry, B.; Wang, Y. Appetite Regulation and Weight Control: The Role of Gut Hormones. *Nutr. Diabetes* **2012**, *2*, No. e26.
(13) De Silva, A.; Bloom, S. R. Gut Hormones and Appetite Control: A Focus on PYY and GLP-1 as Therapeutic Targets in Obesity. *Gut Liver* **2012**, *6*, 10−20.
(14) Greenwood, H. C.; Bloom, S. R.; Murphy, K. G. Peptides and Their Potential Role in the Treatment of Diabetes and Obesity. *Rev. Diabet. Stud.* **2011**, *8*, 355−368.
(15) Steinert, R. E.; Beglinger, C.; Langhans, W. Intestinal GLP-1 and Satiation: From Man to Rodents and Back. *Int. J. Obes.* **2016**, *40*, 198−205.
(16) Karra, E.; Chandarana, K.; Batterham, R. L. The Role of Peptide YY in Appetite Regulation and Obesity. *J. Physiol.* **2009**, *587*, 19−25.
(17) *A Research Study of NNC0165-1875 Alone or Together With Semaglutide in People Who Are Overweight or Obese*. ClinicalTrials.gov, identifier NCT03707990, https://clinicaltrials.gov/ct2/show/NCT03707990, (accessed Mar 2019).
(18) (a) *A Research Study of NNC0165-1875 Alone or Together With Semaglutide in People Who Are Overweight or Obese* ClinicalTrials.gov, identifier NCT03574584, https://clinicaltrials.gov/ct2/show/NCT03574584, (accessed Mar 2019) (b) ClinicalTrials.gov, identifier NCT02568306, https://clinicaltrials.gov/ct2/show/NCT02568306, (accessed Mar 2019).
(19) ClinicalTrials.gov, identifier NCT03490786, https://clinicaltrials.gov/ct2/show/NCT03490786, (accessed Mar 2019).
(20) Tschöp, M.; Castañeda, T. R.; Joost, H. G.; Thöne-Reineke, C.; Ortmann, S.; Klaus, S.; Hagan, M. M.; Chandler, P. C.; Oswald, K. D.; Benoit, S. C.; Seeley, R. J.; Kinzig, K. P.; Moran, T. H.; Beck-Sickinger, A. G.; Koglin, N.; Rodgers, R. J.; Blundell, J. E.; Ishii, Y.; Beattie, A. H.; Holch, P.; Allison, D. B.; Raun, K.; Madsen, K.; Wulff, B. S.; Stidsen, C. E.; Birringer, M.; Kreuzer, O. J.; Schindler, M.; Arndt, K.; Rudolf, K.; Mark, M.; Deng, X. Y.; Withcomb, D. C.; Halem, H.; Taylor, J.; Dong, J.; Datta, R.; Culler, M.; Craney, S.; Flora, D.; Smiley, D.; Heiman, M. L. Does Gut Hormone PYY_{3-36} Decrease Food Intake in Rodents? *Nature* **2004**, *430*, 1−3.
(21) Boggiano, M. M.; Chandler, P. C.; Oswald, K. D.; Rodgers, R. J.; Blundell, J. E.; Ishii, Y.; Beattie, A. H.; Holch, P.; Allison, D. B.; Schindler, M.; Arndt, K.; Rudolf, K.; Mark, M.; Schoelch, C.; Joost, H. G.; Klaus, S.; Thöne-Reineke, C.; Benoit, S. C.; Seeley, R. J.; Beck-Sickinger, A. G.; Koglin, N.; Raun, K.; Madsen, K.; Wulff, B. S.; Stidsen, C. E.; Birringer, M.; Kreuzer, O. J.; Deng, X. Y.; Whitcomb, D. C.; Halem, H.; Taylor, J.; Dong, J.; Datta, R.; Culler, M.; Ortmann, S.; Castañeda, T. R.; Tschöp, M. PYY3-36 as an Anti-Obesity Drug Target. *Obes. Rev.* **2005**, *6*, 307−322.
(22) Ratner, C.; He, Z.; Grunddal, K. V.; Skov, L. J.; Hartmann, B.; Zhang, F.; Feuchtinger, A.; Bjerregaard, A.; Christoffersen, C.; Tschöp, M. H.; Finan, B.; DiMarchi, R. D.; Leinninger, G. M.; Williams, K. W.; Clemmensen, C.; Holst, B. Long-Acting Neurotensin Synergizes with Liraglutide to Reverse Obesity Through a Melanocortin-Dependent Pathway. *Diabetes* **2019**, *68*, 1329−1340.
(23) Kjaergaard, M.; Salinas, C. B. G.; Rehfeld, J. F.; Secher, A.; Raun, K.; Wulff, B. S. PYY(3-36) and Exendin-4 Reduce Food Intake and Activate Neuronal Circuits in a Synergistic Manner in Mice. *Neuropeptides* **2019**, *73*, 89−95.
(24) Rangwala, S. M.; D'Aquino, K.; Zhang, Y. M.; Bader, L.; Edwards, W.; Zheng, S.; Eckardt, A.; Lacombe, A.; Pick, R.; Moreno, V.; Kang, L.; Jian, W.; Arnoult, E.; Case, M.; Jenkinson, C.; Chi, E.; Swanson, R. V.; Kievit, P.; Grove, K.; Macielag, M.; Erion, M. D.; SinhaRoy, R.; Leonard, J. N. A Long-Acting PYY_{3-36} Analog Mediates Robust Anorectic Efficacy with Minimal Emesis in Nonhuman Primates. *Cell Metab.* **2019**, *29*, 837−843.e5.
(25) Dock, S. T.; Carpenter, A. J.; Hunter, III, R. N.; Wu, Y.; Srivastava, V. P. Peptide YY Analogs. *U.S. Patent* US 6,046,167 A *9*, 441023, 2016.
(26) Alexiadou, K.; Anyiam, O.; Tan, T. Cracking the Combination: Gut Hormones for the Treatment of Obesity and Diabetes. *J. Neuroendocrinol.* **2019**, *31*, No. e12664.
(27) Tan, T.; Behary, P.; Tharakan, G.; Minnion, J.; Al-Najim, W.; Albrechtsen, N. J.; Holst, J. J.; Bloom, S. R. The Effect of a Subcutaneous Infusion of GLP-1, OXM, and PYY on Energy Intake and Expenditure in Obese Volunteers. *J. Clin. Endocrinol. Metab.* **2017**, *102*, 2364−2372.
(28) Tan, T. M.; Salem, V.; Troke, R. C.; Alsafi, A.; Field, B. C. T.; De Silva, A.; Misra, S.; Baynes, K. C. R.; Donaldson, M.; Minnion, J.; Ghatei, M. A.; Godsland, I. F.; Bloom, S. R. Combination of Peptide YY_{3-36} with $GLP\text{-}1_{7-36\ amide}$ Causes an Increase in First-Phase Insulin Secretion After IV Glucose. *J. Clin. Endocrinol. Metab.* **2014**, *99*, E2317−E2324.
(29) Schmidt, J. B.; Gregersen, N. T.; Pedersen, S. D.; Arentoft, J. L.; Ritz, C.; Schwartz, T. W.; Holst, J. J.; Astrup, A.; Sjödin, A. Effects of PYY_{3-36} and GLP-1 on Energy Intake, Energy Expenditure, and Appetite in Overweight Men. *Am. J. Physiol. Endocrinol. Metab.* **2014**, *306*, E1248−E1256.
(30) Neary, N. M.; Small, C. J.; Druce, M. R.; Park, A. J.; Ellis, S. M.; Semjonous, N. M.; Dakin, C. L.; Filipsson, K.; Wang, F.; Kent, A. S.; Frost, G. S.; Ghatei, M. A.; Bloom, S. R. Peptide YY_{3-36} and Glucagon-Like $Peptide\text{-}1_{7-36}$ Inhibit Food Intake Additively. *Endocrinology* **2005**, *146*, 5120−5127.
(31) Talsania, T.; Anini, Y.; Siu, S.; Drucker, D. J.; Brubaker, P. L. Peripheral Exendin-4 and Peptide YY^{3-36} Synergistically Reduce Food Intake Through Different Mechanisms in Mice. *Endocrinology* **2005**, *146*, 3748−3756.
(32) Østergaard, S.; Kofoed, J.; Paulsson, J. F.; Grimstrup Madsen, K.; Jorgensen, R.; Wulff, B. S. Design of Y_2 Receptor Selective and Proteolytically Stable PYY_{3-36} Analogues. *J. Med. Chem.* **2018**, *61*, 10519−10530.
(33) Jones, E. S.; Nunn, N.; Chambers, A. P.; Østergaard, S.; Wulff, B. S.; Luckman, S. M. Modified Peptide YY Molecule Attenuates the Activity of NPY/AgRP Neurons and Reduces Food Intake in Male Mice. *Endocrinology* **2019**, *160*, 2737−2747.
(34) Nishizawa, N.; Niida, A.; Adachi, Y.; Masuda, Y.; Kumano, S.; Yokoyama, K.; Asakawa, T.; Hirabayashi, H.; Amano, N.; Takekawa, S.; Ohtaki, T.; Asami, T. Potent Antiobesity Effect of a Short-Length Peptide YY-Analogue Continuously Administered in Mice. *Bioorg. Med. Chem. Lett.* **2017**, *27*, 3829−3832.
(35) Nishizawa, N.; Niida, A.; Adachi, Y.; Kanematsu-Yamaki, Y.; Masuda, Y.; Kumano, S.; Yokoyama, K.; Noguchi, Y.; Asakawa, T.; Hirabayashi, H.; Amano, N.; Takekawa, S.; Ohtaki, T.; Asami, T. Highly Potent Antiobesity Effect of a Short-Length Peptide YY Analog in Mice. *Bioorgan. Med. Chem.* **2017**, *25*, 5718−5725.

https://dx.doi.org/10.1021/acs.jmedchem.0c00740
J. Med. Chem. XXXX, XXX, XXX−XXX

(36) Balasubramaniam, A.; Joshi, R.; Su, C.; Friend, L. A.; James, J. H. Neuropeptide Y (NPY) Y_2 Receptor-Selective Agonist Inhibits Food Intake and Promotes Fat Metabolism in Mice: Combined Anorectic Effects of Y_2 and Y_4 Receptor-Selective Agonists. *Peptides* **2007**, *28*, 235−240.
(37) Balasubramaniam, A.; Tao, Z.; Zhai, W.; Stein, M.; Sheriff, S.; Chance, W. T.; Fischer, J. E.; Eden, P. E.; Taylor, J. E.; Liu, C. D.; McFadden, D. W.; Voisin, T.; Roze, C.; Laburthe, M. Structure−Activity Studies Including a $\psi(CH_2\text{-}NH)$ Scan of Peptide YY (PYY) Active Site, PYY(22−36), for Interaction with Rat Intestinal PYY Receptors: Development of Analogues with Potent In Vivo Activity in the Intestine. *J. Med. Chem.* **2000**, *43*, 3420−3427.
(38) Niida, A.; Kanematsu-Yamaki, Y.; Asakawa, T.; Ishimura, Y.; Fujita, H.; Matsumiya, K.; Nishizawa, N.; Adachi, Y.; Mochida, T.; Tsuchimori, K.; Yoneyama-Hirozane, M.; Sakamoto, J.; Hirabayashi, H.; Fukui, H.; Takekawa, S.; Asami, T. Antiobesity and Emetic Effects of a Short-Length Peptide YY Analog and its PEGylated and Alkylated Derivatives. *Bioorg. Med. Chem.* **2018**, *26*, 566−572.
(39) DeCarr, L. B.; Buckholz, T. M.; Milardo, L. F.; Mays, M. R.; Ortiza, A.; Lumb, K. J. A Long-Acting Selective Neuropeptide Y2 Receptor PEGylated Peptide Agonist Reduces Food Intake in Mice. *Bioorg. Med. Chem. Lett.* **2007**, *17*, 1916−1919.
(40) Hutchinson, J. A.; Burholt, S.; Hamley, I. W.; Lundbank, A. K.; Uddin, S.; Gomes dos Santos, A.; Reza, M.; Seitsonen, J.; Ruokolainen, J. The Effect of Lipidation on the Self-Assembly of the Gut-Derived Peptide Hormone PYY_{3-36}. *Bioconjugate Chem.* **2018**, *29*, 2296−2308.
(41) Castelletto, V.; Hamley, I. W.; Seitsonen, J.; Ruokolainen, J.; Harris, G.; Bellman-Sickert, K.; Beck-Sickinger, A. G. Conformation and Aggregation of Selectively PEGylated and Lipidated Gastric Peptide Hormone Human PYY_{3-36}. *Biomacromolecules* **2018**, *19*, 4320−4332.
(42) Yang, P.-Y.; Zou, H.; Chao, E.; Sherwood, L.; Nunez, V.; Keeney, M.; Ghartey-Tagoe, E.; Ding, Z.; Quirino, H.; Luo, X.; Welzel, G.; Chen, G.; Singh, P.; Woods, A. K.; Schultz, P. G.; Shen, W. Engineering a Long-Acting, Potent GLP-1 Analog for Microstructure-Based Transdermal Delivery. *Proc. Natl. Acad. Sci. USA* **2016**, *113*, 4140−4145.
(43) Yang, P.-Y.; Zou, H.; Lee, C.; Muppidi, A.; Chao, E.; Fu, Q.; Luo, X.; Wang, D.; Schultz, P. G.; Shen, W. Stapled, Long-Acting Glucagon-Like Peptide 2 Analog with Efficacy in Dextran Sodium Sulfate Induced Mouse Colitis Models. *J. Med. Chem.* **2018**, *61*, 3218−3223.
(44) Muppidi, A.; Zou, H.; Yang, P.-Y.; Chao, E.; Sherwood, L.; Nunez, V.; Woods, A. K.; Schultz, P. G.; Lin, Q.; Shen, W. Design of Potent and Proteolytically Stable Oxyntomodulin Analogs. *ACS Chem. Biol.* **2016**, *11*, 324−328.
(45) Pflimlin, E.; Lear, S.; Lee, C.; Yu, S.; Zou, H.; To, A.; Joseph, S.; Nguyen-Tran, V.; Tremblay, M. S.; Shen, W. Design of a Long-Acting and Selective MEG-Fatty Acid Stapled Prolactin-Releasing Peptide Analog. *ACS Med. Chem. Lett.* **2019**, *10*, 1166−1172.
(46) Lear, S.; Amso, Z.; Shen, W. Engineering PEG-Fatty Acid Stapled, Long-Acting Peptide Agonists for G Protein-Coupled Receptors. *In Methods in Enzymology* **2019**, *622*, 183−200.
(47) (a) Nygaard, R.; Nielbo, S.; Schwartz, T. W.; Poulsen, F. M. The PP-Fold Solution Structure of Human Polypeptide YY and Human PYY3-36 as Determined by NMR. *Biochemistry* **2006**, *45*, 8350−8357. (b) Kaiser, A.; Müller, P.; Zellmann, T.; Scheidt, H. A.; Thomas, L.; Bosse, M.; Meier, R.; Meiler, J.; Huster, D.; Beck-Sickinger, A. G.; Schmidt, P. Unwinding of the C-Terminal Residues of Neuropeptide Y is Critical for Y_2 Receptor Binding and Activation. *Angew. Chem., Int. Ed.* **2015**, *54*, 7446−7449.
(48) Schrödinger, L. L. C. *The PyMOL Molecular Graphics System*; Version 1.6 Schrödinger.
(49) Lau, J.; Bloch, P.; Schäffer, L.; Pettersson, I.; Spetzler, J.; Kofoed, J.; Madsen, K.; Knudsen, L. B.; McGuire, J.; Steensgaard, D. B.; Strauss, H. M.; Gram, D. X.; Knudsen, S. M.; Nielsen, F. S.; Thygesen, P.; Reedtz-Runge, S.; Kruse, T. Discovery of the Once-Weekly Glucagon-Like Peptide-1 (GLP-1) Analogue Semaglutide. *J. Med. Chem.* **2015**, *58*, 7370−7380.
(50) Pedragosa-Badia, X.; Stichel, J.; Beck-Sickinger, A. G. Neuropeptide Y Receptors: How to Get Subtype Selectivity. *Front. Endocrinol.* **2013**, *4*, 5.
(51) Kanoski, S. E.; Rupprecht, L. E.; Fortin, S. M.; De Jonghe, B. C.; Hayes, M. R. The Role of Nausea in Food Intake and Body Weight Suppression by Peripheral GLP-1 Receptor Agonists, Exendin-4 and Liraglutide. *Neuropharmacology* **2012**, *62*, 1916−1927.
(52) Halatchev, I. G.; Cone, R. D. Peripheral Administration of PYY_{3-36} Produces Conditioned Taste Aversion in Mice. *Cell Metab.* **2005**, *1*, 159−168.
(53) Muppidi, A.; Lee, S. J.; Hsu, C.-H.; Zou, H.; Lee, C.; Pflimlin, E.; Mahankali, M.; Yang, P.-Y.; Chao, E.; Ahmad, I.; Crameri, A.; Wang, D.; Woods, A.; Shen, W. Design and Synthesis of Potent, Long-Acting Lipidated Relaxin-2 Analogs. *Bioconjugate Chem.* **2019**, *30*, 83−89.

https://dx.doi.org/10.1021/acs.jmedchem.0c00740
J. Med. Chem. XXXX, XXX, XXX−XXX